The catalytic site of serine proteinases as a specific binding cavity for xenon

Marc Schiltz[1]*, Roger Fourme[1], Isabelle Broutin[2] and Thierry Prangé[1,3]

[1]LURE (CNRS, CEA, MESR), Université Paris-Sud, Bât.209d, 91405 Orsay Cedex, France, [2]Laboratoire de Biologie Structurale (CNRS), 91198 Gif sur Yvette, France and [3]Chimie Structurale Biomoléculaire (URA 1430 CNRS), 74 rue M. Cachin, 93012 Bobigny Cedex, France

Background: Under moderate pressure, xenon can bind to proteins and form weak but specific interactions. Such protein–xenon complexes can be used as isomorphous derivatives for phase determination in X-ray crystallography.

Results: Investigation of the serine proteinase class of enzymes shows that the catalytic triad, the common hydrolytic motif of these enzymes, is a specific binding site for one xenon atom and shows high occupancy at pressures below 12 bar. Complexes of xenon with two different serine proteinases, elastase and collagenase, were analyzed and refined to 2.2 Å and 2.5 Å resolution, respectively. In both cases, a single xenon atom with a low temperature factor is located in the active site at identical positions. Weak interactions exist with several side chains of conserved amino acids at the active site. Xenon binding does not induce any major changes in the protein structure and, as a consequence, crystals of the xenon complexes are highly isomorphous with the native protein structures. Xenon is also found to bind to the active site of subtilisin Carlsberg, a bacterial serine proteinase, that also has a catalytic triad motif.

Conclusions: As the region around the active site shows conserved structural homology in all serine proteinases, it is anticipated that xenon binding will prove to be a general feature of this class of proteins.

Structure 15 March 1995, **3**:309–316

Key words: collagenase, porcine pancreatic elastase, serine proteinases, subtilisin Carlsberg, xenon, X-ray diffraction

Introduction

Xenon is a relatively water-soluble noble gas [1]. Despite its inert behaviour, it has been observed to exert a weak anaesthetic effect when injected into the blood stream [2]. In nuclear medicine, ^{133}Xe is used to study cerebral blood flow and pulmonary function [3]. Also, in a recent study, it has been shown that ^{129}Xe polarized by laser-light can be used very effectively for high-resolution magnetic resonance imaging in living organisms [4].

In addition to its numerous covalent chemical derivatives with fluorine and oxygen, xenon is known to bind non-covalently to a number of small organic molecules [5] and also to proteins, including myoglobin [6] and haemoglobin [7]. These protein–xenon complexes can be used as heavy-atom derivatives for determining single isomorphous replacement with anomalous scattering (SIRAS) phases in macromolecular X-ray crystallography [8]. The experimental procedure for preparing xenon complexes of macromolecular crystals has recently been re-investigated [9]. The outcome is a convenient way of testing for the ability of this kind of exotic heavy atom to bind to proteins. Here, this same method has been tested on two different eukaryotic serine proteinases: porcine pancreatic elastase (PPE) and collagenase from *Hypoderma lineatum* (HLC), the latter crystallizing as a dimer.

Serine proteinases are a group of enzymes that hydrolyze peptide bonds in proteins and participate in a broad range of physiological processes. They are present in all forms of living organisms and, because of their biological importance, they have been extensively studied by structural methods, including X-ray crystallography (for a review, see [10]).

The refined structures of xenon complexes obtained at pressures of 8 bar (for PPE) and 12 bar (for HLC) are described. In both cases, xenon is found to bind at the active site of the enzymes. In addition, the binding of xenon to the active site of subtilisin Carlsberg from *Bacillus licheniformis* (at a gas pressure of 12 bar) is reported.

Results and discussion

Location of xenon atoms

Xenon atoms were located by difference-Fourier calculations using the terms $F_{deriv}-F_{nat}$, as amplitudes. The phases were computed from refined native structures, using known coordinates deposited with the protein data bank [11]. (Coordinates have not yet been submitted for HLC and so were obtained from [12,13].) In both cases, very clean difference maps were obtained. For PPE, a single spherical peak with maximum density of 31σ (where σ is the root mean square of the whole map density) is observed. In the case of HLC, two spherical peaks at 44σ and 39σ, respectively, are observed (Fig. 1). Apart from these peaks, both maps are essentially featureless and the next highest-ranked peaks do not exceed the 5σ

*Corresponding author.

Fig. 1. Cα backbone chain of the native HLC dimer superposed on a 2.5 Å resolution (F_{Xe}–F_{nat}) difference-Fourier map. The map is contoured at the 5σ level (where σ is the root mean square of the whole map density). Both peaks (with maximum densities of 44σ and 39σ, respectively) correspond to single xenon atoms (shown in pink) bound in the active site of each monomer

level. In both subunits of the HLC dimer, and in PPE, the xenon atoms are located at almost identical positions, namely in the active site, close to the catalytic serine residue (Ser195 in the standard chymotrypsinogen numbering). Fig. 2 shows the location of xenon in PPE.

Structure refinements

Crystallographic refinements were carried out by the technique of simulated annealing [14] with the X-PLOR program [15]. The final stages were carried out by restrained least-squares refinement using the PROLSQ program [16].

The native structures of PPE and HLC inclusive of the previously located xenon atoms but exclusive of water molecules, were used as starting models. The initial R-factors were 0.35 for PPE and 0.29 for HLC. (The R-factor is defined as being the normalized crystallographic residual:

$$R=\Sigma_{h,k,l}\,|\,|F_{obs}(h,k,l)|-k|F_{calc}(h,k,l)|\,|\,/\Sigma_{h,k,l}|F_{obs}(h,k,l)|$$

where h,k,l are the reciprocal lattice points of the crystal, $|F_{obs}(h,k,l)|$ and $|F_{calc}(h,k,l)|$ are the observed and calculated structure-factor amplitudes, respectively, and k is a scale factor.) Refinements started at a limited resolution of 3 Å and were gradually extended to the maximum resolution of the measured data (2.2 Å for PPE and 2.5 Å for HLC). Difference-Fourier maps were calculated and used to determine the positions of water molecules. Water molecules were gradually added and refined. Most of them corresponded to within 0.5–1 Å of the original water molecule positions in the native structures. Notable exceptions were those that were previously in the active sites, and had now been displaced by the xenon atoms. The final R-factors are 0.172 (PPE) and 0.178 (HLC) for all structure-factor amplitudes above two standard deviations. The average statistics on distances for bond lengths, angles, planes, chiral volumes and isotropic temperature factors are reported in Table 1. Simultaneous refinement of occupancies and temperature factors for the xenon atoms is difficult: not only do the results depend on the force field used for calculating refinement constraints, but also both parameters are not completely uncorrelated if the resolution of the data is limited. Initial trials converged to occupancies higher than 1.0. This observation, together with the fact that the xenon peaks in the difference-Fourier maps are very intense, led us to fix occupancies at 1.0 and to freely refine temperature factors.

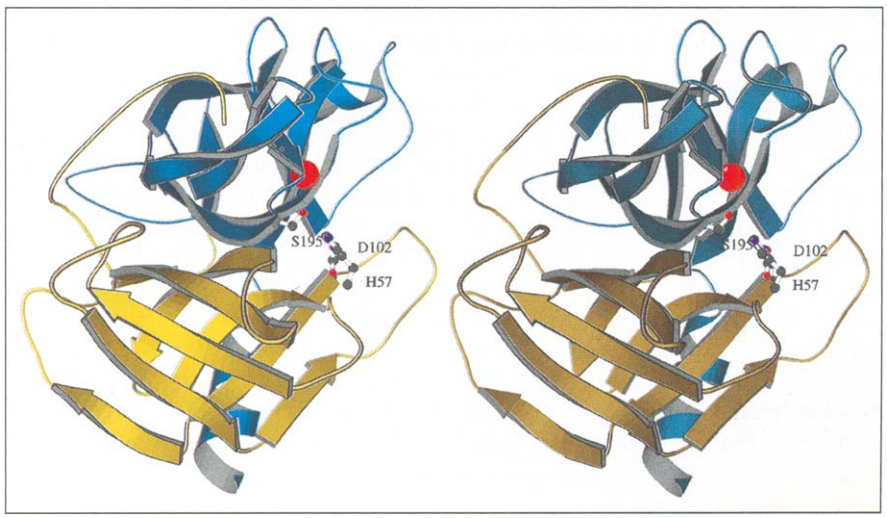

Fig. 2. Stereoview of the Cα backbone chain of PPE showing the position of the bound xenon atom (in red colour). The two antiparallel β-barrel domains are displayed in blue and yellow colours, respectively. Also displayed are the side chains of the residues belonging to the catalytic triad.

Table 1. Final rms values at the end of structure refinements.

Constraints	PPE	HLC	
Bond distances (1–2) Å	0.011 (1870)	0.012 (3646)	
Angle distances (1–3) Å	0.028 (2559)	0.034 (4980)	
Planar distances (1–4) Å	0.036 (680)	0.047 (1326)	
Planes (Å)	0.012 (322)	0.013 (628)	
Chiral volumes (Å^3)	0.07 (289)	0.07 (554)	
Single contact torsions (Å)	0.19 (418)	0.203 (902)	
Multiple contact torsions (Å)	0.27 (873)	0.27 (2948)	
Hydrogen bonds (Å)	0.16 (174)	0.24 (542)	
Planar angles (ω etc)	3.2° (251)	2.8° (470)	
Staggered (±60, 180°)	18° (287)	18° (572)	
Orthonormal (±90°)	21° (27)	21° (56)	
		A[a]	B[b]
Average B-factors (Å^2):			
Main-chain	7.7 (961)	25.5 (921)	30.5 (921)
Side-chain	11.3 (861)	28.1 (857)	32.3 (857)
Water molecules	26.1 (125)	44.1 (295)	
R-factor	0.172	0.178	
Weights in R-factor	94–100[a] (s-1/6)	185–221[a] (s-1/6)	
Rms shifts in last cycle:			
Coordinates (Å)	0.015	0.014	
B-factors (Å^2)	1.8	1.2	
No. of F_{obs} used	10801	17087	
Resolution range (Å)	10–2.2	12–2.5	
Xenon atoms:			
B-factor (Å^2)	20.1	24.8	30.5
Fractional coordinates			
x	0.217	0.198	0.285
y	0.939	0.426	0.254
z	0.990	0.195	0.120

Abbreviations: PPE, porcine pancreatic elastase; HLC *Hypoderma lineatum* collagenase. The number of parameters used in each refinement are shown in parentheses. [a]Subunit A, [b]Subunit B.

Comparison between native and derivative structures

Xenon fixation does not induce any major structural change. The root mean square deviations (rmsds) between the positions of corresponding atoms, in the native structures and in the xenon complexes, are relatively small. For backbone atoms, the average values are 0.07 Å for PPE and 0.09 Å for HLC. The largest side-chain deviations (<0.20 Å for PPE, and <0.25 Å for HLC) occur mainly for residues at the protein surface. The rmsds for subunit A of HLC are shown in Fig. 3. These results confirm the earlier findings, from myoglobin [17], that xenon complexes exhibit a high degree of isomorphism with the corresponding native structures.

Binding of xenon in the pocket of the catalytic site

The active site of serine proteinases has been widely analyzed [10,18]. It comprises an activated serine (Ser195) assisted by a proton relay (His57), which acts as a general base. The imidazole of the active-site histidine is stabilized by hydrogen bonds to an aspartic acid (Asp102). These three residues are brought together by protein folding in a motif known as a catalytic triad. The mechanism by which serine proteinases hydrolyze bonds has been intensively studied and is now well understood. The specificity of these enzymes for a given amide bond (or ester bond in the case of esterases) arises more from the protein folding, and the character of the residues building the substrate-binding pocket, than from the catalytic triad itself, which in all structures displays a remarkably constant three-dimensional configuration.

The two enzymes selected in this study have different topologies and specificities. While PPE has a narrow active site, HLC, which crystallizes as a dimer, has a more elongated active site that is closed by a two stranded β-sheet; this comes from the other HLC monomer in a symmetrical arrangement [12].

The refined structures of the enzymes complexed with xenon show that there is only one xenon site per enzyme molecule. All sites have high occupancies in the pressure range studied. In all cases, the xenon atom is located at a position which is approximately midway between the catalytic serine residue (Ser195) and the so-called primary specificity pocket (S1, consisting of residues Thr213–Val216, Thr226 and Val227, according to the numbering system given in [19]) (Figs. 4,5). In the native structure of PPE, the xenon-binding site is occupied by a water molecule (this water molecule has been labelled Sol-552 in the description of the native PPE structure [19]). The water molecule is in close contact with Oγ(Ser195) and with the carbonyl oxygen of residue 191. In the structure of a complex formed between peptidyl α,α-difluoro-β-keto amide and PPE [20], the xenon-binding site is occupied by the Cβ of a valine residue whose carbonyl carbon atom is covalently bound to Oγ(Ser195).

The side-chain oxygen of Ser195 is well oriented for creating a weak interaction without modification of its

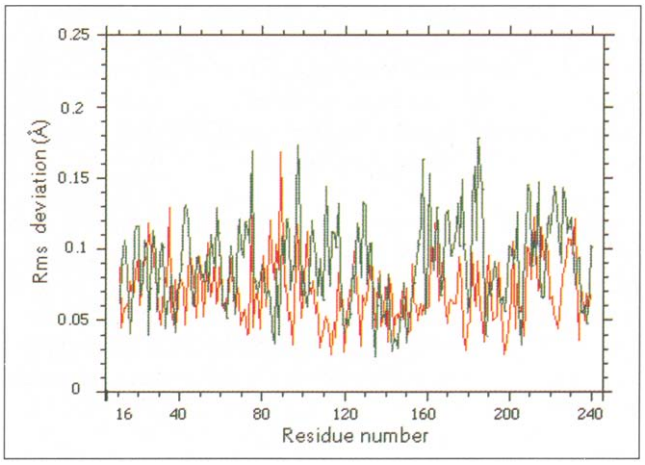

Fig. 3. Rms deviations between the native structure and the xenon complex for subunit A of HLC. Main chains are shown in red and side chains in green lines.

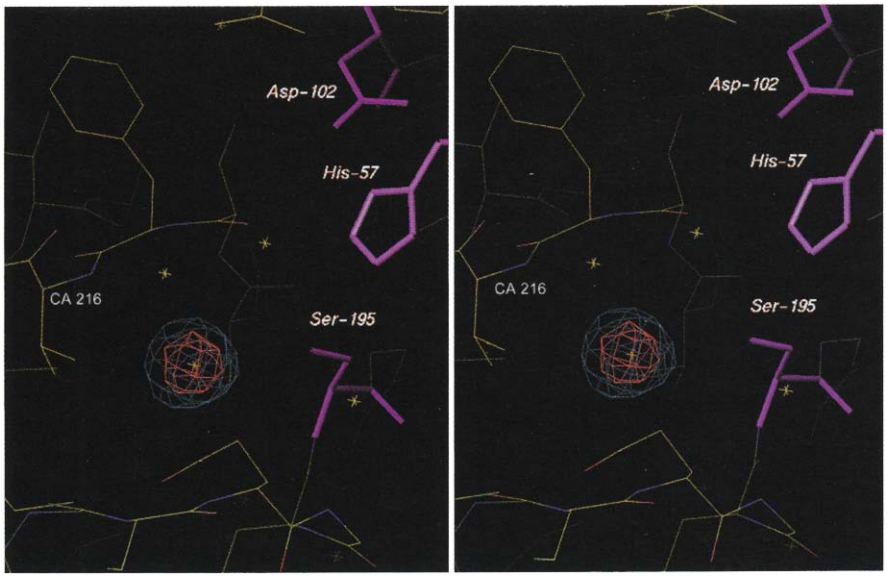

Fig. 4. Close-up stereoview of the active site region of PPE. The refined structure of the xenon complex is superposed on a 2.2 Å resolution (F_{Xe}–F_{nat}) difference-Fourier map. The map is contoured at the 10σ (blue) and at the 20σ (red) levels (where σ is the rms of the whole map density). The single spherical peak (with maximum density of 31σ) corresponds to a xenon atom bound into the active site. Also displayed (pink) are the side chains of the residues belonging to the catalytic triad.

conformation. Thus, in all three cases (PPE, HLC subunits A and B), Oγ(Ser195) is the non-hydrogen atom that is closest to the xenon atom. The geometry of the xenon atom and its closest neighbouring atoms (Table 2) is similar in the three molecules: the Oγ(Ser195)-Xe-Cγ2(Val216) angle is nearly linear, with the other 'ligands' being in a plane which is roughly perpendicular to that axis. Xenon atoms have a van der Waals radius of 2.09 Å. The distances between xenon and its closest neighbours are slightly greater than the sums of the corresponding van der Waals radii. Consequently, xenon inserts itself into the active site without any further perturbation of the protein structure. Xenon binding does not disturb the catalytic triad: the pre-existing hydrogen bond between Ser195 and His57 is still present (3.2 Å, 2.7 Å and 2.7 Å in PPE, HLC subunits A and B, respectively) with a serine χ angle of −58°, −66° and −69° in the three structures.

It is, however, surprising how tightly the xenon atoms are bound. This point is illustrated by the PPE structure which also contains a calcium ion located in an aspartic-acid-rich region. After the refinement process, when the thermal factor constraints on individual atoms are released, the xenon atom is found to be more ordered (B=20.1 Å^2) than the doubly charged calcium ion (B=27 Å^2), which is bound by strong electrostatic interactions.

Inspection of the crystal structure shows that, in the case of HLC, the active site is not freely accessible. In fact, for each molecule, the cleft leading to the catalytic cavity is closed by a two-stranded β-sheet from the other monomer in the asymmetric unit. Xenon binding must therefore involve dynamic fluctuations of the protein structure by which access to the active site is possible.

Binding of xenon to metmyoglobin was previously analyzed in detail [17]. Four binding sites with varying occupancies were observed at a pressure of 7 bar. They are located in essentially pre-existing cavities that are built by hydrophobic residues. Tilton *et al.* [17] pointed out that, in the absence of xenon atoms, the cavities are void — that is, they found no evidence of water molecules being bound in these cavities. In contrast to these observations, we find that, in PPE and HLC, the binding sites exhibit hydrophilic character. In the refined structures of native PPE and HLC, water molecules are

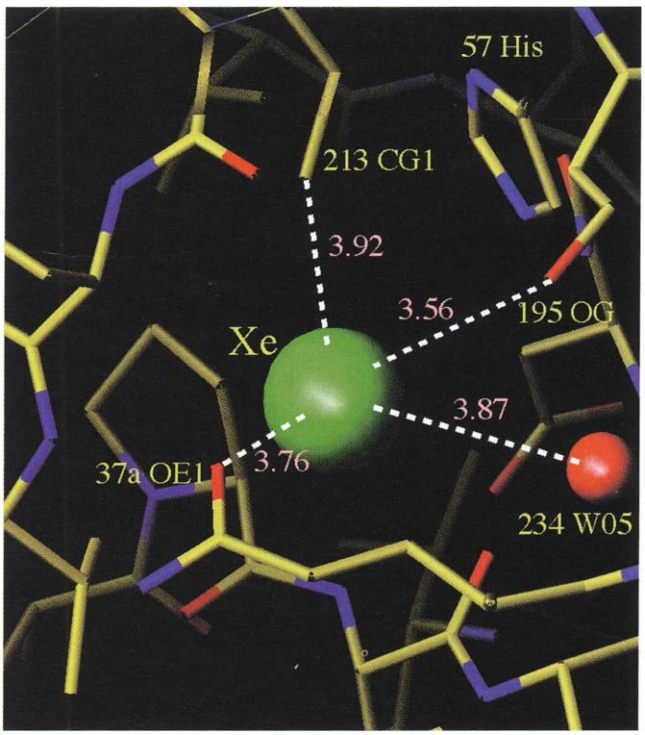

Fig. 5. Close-up view of the active site region of the refined structure of the xenon complex of HLC (subunit A). The xenon atom is displayed as a green-coloured sphere. Water molecules are displayed as red-coloured spheres. Also displayed are the interactions with atoms in the 4 Å range. The catalytic Ser195 Oγ atom is closest to xenon, with a distance of 3.56 Å. The catalytic His57 is located in the upper right corner, just above Ser195.

Table 2. Closest contacts within the range 3.1–4.4 Å (around the xenon atom in the three analyzed active sites (all values in Å).

	PPE	HLC subunit A	HLC subunit B
Xe-O (Cys191)	3.7	4.4	4.4
Xe-Oγ (Ser195)	3.4	3.6	3.7
Xe-Cγ2 (Val216)	3.9	4.0	3.8
Xe-Oε1 (Gln37)[a]	[b]	3.8	4.0
Xe-Cγ2 (Thr213)	4.0	–	–
Xe-Cγ1 (Val213)	–	3.9	3.8
Xe-WO5 (W234)	[b]	3.9	4.4

Residue numbering follows the standard chymotrypsinogen labelling. [a]From the other subunit of HLC. [b]Not observed in PPE.

located near or very close to the xenon-binding sites: one in PPE (Sol-552) and two in each subunit of HLC. In the complex of PPE, the water molecule is no longer present after xenon binding, while in HLC a single water molecule (Sol-234) is observed, displaced 4 Å away from the position of a water molecule in the native structure, and remaining in the vicinity of the xenon atom (Table 2). It may at first sight look surprising that favourable hydrogen bonds with bound water molecules are sacrificed for, the generally weaker, Debye and London interactions with xenon atoms. However, it has to be remembered that, upon release from the protein, a water molecule re-establishes strong hydrogen bonds with the bulk solvent. Thus, in some cases, the energy gap between binding and releasing of water molecules may be small and xenon binding may indeed compensate for the loss of water.

Whilst in the case of metmyoglobin, xenon binding mainly involves London interactions [21], the environment of the active site in serine proteinases comprises a number of polar groups such that dipole-induced interactions presumably also play an important role. As the polarizability of xenon is particularly high [7], this may at least give a qualitative answer to why xenon binding in the active site is favoured. The electrostatic environment created by the neighbouring polar groups, as well as the size and the form of the binding cavity, may all influence the thermodynamics of xenon binding. We are currently carrying out detailed investigations into the role played by each of these factors. The results of these investigations, which will also include cases other than serine proteinases, will be presented in a future communication.

Binding of xenon to subtilisin Carlsberg from *B. licheniformis*

The region around the catalytic site is known to show conserved structural homology in all eukaryotic serine proteinases. In particular, the side chains of the residues belonging to the catalytic triad have the same three-dimensional arrangement in all members of this protein class. Given these facts, and results obtained on PPE and HLC, it might be anticipated that xenon binding is a general feature which holds for most (if not all) serine proteinases. To verify this hypothesis, we tested xenon binding to crystals of subtilisin Carlsberg from *B. licheniformis*.

The subtilisins are proteolytic enzymes of bacterial origin whose active site is composed of a catalytic triad (Ser–His–Asp) which exhibits the same geometry as those of eukaryotic serine proteinases. The other side chains and the direction of the main chains carrying the triad, are very different in orientation. Whereas the structure of eukaryotic serine proteinases consists basically of two antiparallel β-barrel domains, the structure of subtilisins is made up of a parallel β-sheet surrounded by α-helices [22,23]. Since, apart from the catalytic site, there is no structural similarity between these two classes of enzymes, they have become one of the best known examples at the molecular level of what is called 'convergent evolution' [24]. Thus, subtilisin Carlsberg may be used to test, firstly, if xenon binding is essentially controlled by the environment of the catalytic triad, and secondly, if xenon binding is a common feature of all serine proteinases.

A difference-Fourier map of a 12 bar xenon derivative of subtilisin Carlsberg exhibits a prominent spherical peak with a maximum density of 21σ (Fig. 6). Once again, the peak is located in the active site, with its centre being at a distance of approximately 4.2 Å from the Oγ atom of the catalytic serine residue (Ser221). This result suggests that the ability to bind xenon in the active site is a common feature of all serine proteinases.

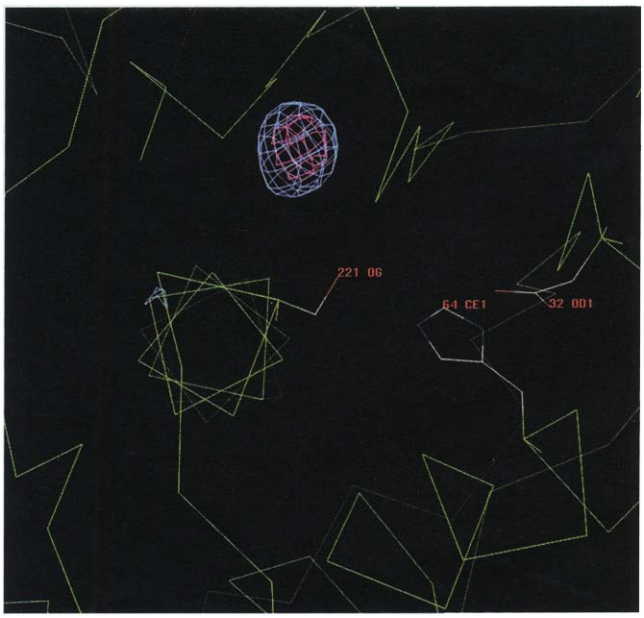

Fig. 6. Close-up view of the active site region of subtilisin Carlsberg from *B. licheniformis*. The Cα backbone chain (green) of the native structure is superposed on a 2.2 Å resolution (F_{Xe}–F_{nat}) difference-Fourier map. The map is contoured at the 8σ (blue) and at the 14σ (pink) levels (where σ is the rms of the whole map density). The single spherical peak (with maximum density of 21σ) corresponds to a xenon atom bound into the active site. Also displayed are the side chains of the residues belonging to the catalytic triad.

Table 3. Experimental details of data collections.

	PPE		HLC		Subtilisin Carlsberg	
	Native	Xe (8 bar)	Native	Xe (12 bar)	Native	Xe (12 bar)
Space group	$P2_12_12_1$		I422		$P2_12_12_1$	
Cell parameters (in Å)	a=50.91 b=57.84 c=74.72	a=50.66 b=57.68 c=74.75	a=b=111.7 c=165.8	a=b=111.35 c=165.09	a=76.22 b=55.03 c=52.67	a=76.19 b=55.18 c=52.48
No. of measured reflections	90636	45968	202947	116536	40951	39865
No. of unique reflections	11988	10937	41609	17432	11262	7865
Resolution limits (in Å)	17.7–2.15	17.7–2.20	25–1.75	14.4–2.53	11.89–2.16	11.89–2.15
R_{merge}[a]	0.072	0.051	0.070	0.081	0.058	0.037
R_{iso} (native/Xe)[b]	0.127		0.164		0.104	

[a]The R_{merge} is defined as $\Sigma_h\Sigma_i|<I(h)>-I_i(h)|/\Sigma_h\Sigma_iI_i(h)$ where $I_i(h)$ is the i^{th} intensity measurement of reflection h. [b]The r_{iso} is defined as $\Sigma_h|F_{nat}(h)-F_{deriv}(h)|/\Sigma_hF_{nat}(h)$ where $F_{nat}(h)$ and $F_{deriv}(h)$ are the measured structure-factor amplitudes of reflection h for the native and xenon derivative structures, respectively.

Conclusion

Xenon has been studied extensively, both theoretically and experimentally, as a prototype gas, liquid and solid [25] and much is known about its interactions and properties. Xenon appears, therefore, to be an ideal probe for investigating ligand-binding properties of proteins. First principles of thermodynamics dictate that, at equilibrium, the chemical potential of xenon in the gas phase must equal the chemical potential of xenon bound to the protein. These chemical potentials can, in principle, be derived from molecular properties. The simplicity of the probe, a single atom, should allow one to carry out molecular-dynamics simulations and theoretical computations in a much more straightforward manner than is possible with more complex ligands. Detailed studies of protein–xenon complexes might therefore lead to a better understanding of interactions between proteins and ligands, and eventually bridge the gap between experimental findings and thermodynamic theories.

As xenon binding is controlled by protein motions, xenon might also serve as a probe for studying protein dynamics. Such investigations have been carried out by NMR studies of ^{129}Xe binding of myoglobin and haemoglobin [26]. The advantages of xenon in NMR studies have been reviewed [27]: natural xenon contains the two NMR-sensitive isotopes, ^{129}Xe (spin 1/2) and ^{131}Xe (spin 3/2) in high abundance. The very different relaxation times of these two isotopes make them complementary for time-resolved NMR studies.

Perhaps the most important application of xenon complexes is in the field of protein crystallography. Despite the emergence of a number of new techniques for phase determination over the last decade, the method of isomorphous replacement still remains the most powerful one in the case of proteins for which no model is available. However, the difficulty in obtaining heavy-atom derivatives sufficiently isomorphous with the native structures, limits the effectiveness of this method. The unique advantages of xenon derivatives — among which the most important ones are their high degree of isomorphism and their anomalous scattering properties — have recently been reviewed [9].

The results of the present study suggest that structure determination via isomorphous replacement with xenon derivatives could be straightforward for proteins of the serine proteinase family. It might also be expected that xenon binding may be observed in other important enzyme classes that are characterized by catalytic sites of a related topology such as esterases, lipases or cysteine proteinases. After the initial submission of this manuscript, we tested whether xenon also binds to *Fusarium solani pisi* cutinase. Cutinase is not a serine proteinase but a lipolytic esterase which hydrolyzes triglycerides. It is an α-β protein whose catalytic site is composed of a Ser–His–Asp triad [28]. Once more, xenon is found to bind in the active site, close to the catalytic serine residue (Schiltz, M, Fourme, R, Martinez, C, Longhi, S, Cambillau, C & Prangé, T, unpublished data). This result lends further support to the hypothesis that xenon binding into the active site is a fairly general feature for serine hydrolases.

In a further development, we have been able to show that krypton also binds into the active site of PPE. Although krypton is not very useful as heavy atom (due to its low atomic number) its K absorption edge is at 0.865 Å, which is readily accessible on synchrotron radiation sources, thus allowing one to exploit the changes in its anomalous scattering properties near this edge (Schiltz, M, Fourme, R, Shepard, W & Prangé, T, unpublished data).

Biological implications

In this study, it has been shown that the noble gas, xenon, can bind into the active site of serine proteinases with minimal perturbation of the protein structure. Interactions of xenon with biomolecules have led to important applications in nuclear

medicine [3], in magnetic resonance imaging of living organisms [4] and in experimental anaesthesiology [2].

Serine proteinases fulfil many important physiological functions, ranging from generalized protein digestion to more specific regulated processes such as blood coagulation. Many efforts have been made to determine the atomic structure of serine proteinases and to understand their biological function at the molecular level. A great deal of the current structural knowledge in enzymology and, more generally in molecular biology, has come from X-ray crystallographic studies. Yet, despite constant progress over the last 40 years, crystallographic determination of macromolecular structures is still far from being a routine task. At present, the major obstacle to this goal is the well-known phase problem, which arises from the fact that a diffraction experiment on a crystal yields the amplitudes, but not the phases, of diffracted waves. In this context, heavy-atom derivatives are of paramount importance for solving the phase problem by the method of isomorphous replacement.

In this study, xenon derivatives of two eukaryotic serine proteinases, elastase and collagenase, have been characterized. Xenon was also found to bind to a member of the subtilisin family. Both classes of enzymes fulfil similar biological functions, but apart from the catalytic triad, they have completely different structures. It is precisely in the region of the catalytic site that xenon is found to bind. It is therefore expected that xenon binding will be a general feature of serine proteinases. Furthermore, it might be anticipated that xenon derivatives could be obtained with other proteins that contain catalytic triads. Four groups of enzymes that contain catalytic Glu/Asp–His–Ser/Cys triads have been identified: eukaryotic serine proteinases, cysteine proteinases, subtilisins and the α/β-hydrolase superfamily (which comprises, among others, acetylcholine esterases, thioesterases, serine carboxypeptidases and lipases) [29]. These enzymes have no structural similarity apart from the catalytic triad at the active site and therefore it is thought that this stable active site must have arisen via convergent evolution. Phase determination with xenon derivatives might yield essential structural information for a number of these very important enzymes.

Materials and methods

Crystal preparation

Lyophilized PPE from SERVA Chemicals was used without further purification. Single crystals of PPE were grown at 18°C by the batch method, using Na_2SO_4 as the crystallizing agent according to conditions described in [30]. Lyophilized subtilisin Carlsberg from *B. licheniformis* was purchased from SIGMA Chemicals and used without further purification. Single crystals were grown at 18°C by the micro-dialysis method, using Na_2SO_4 as the crystallizing agent [31].

HLC was isolated and purified at the Institut Pasteur [32] and crystallized by Ducruix *et al.* [33]. Crystals were grown at 18°C by the hanging-drop vapor diffusion method, using $(NH_3)_2SO_4$ as the crystallizing agent. The method used to prepare xenon derivatives has been previously described [9]: native crystals, mounted in a quartz capillary fitted to a specially designed cell, were pressurized with xenon gas at 8 bar for PPE and 12 bar for HLC and subtilisin Carlsberg.

X-ray data collection and processing

Native and derivative data were collected under nearly identical conditions. Details are given in Table 3. Data were collected at station DW32 of the wiggler beam line at the LURE-DCI synchrotron (Orsay, France) [34] with monochromated X-rays, λ=0.90 Å. A MAR-Research imaging-plate system was used as detector. Crystals were maintained at a temperature of 18°C throughout data collection. For xenon derivatives, each collection started 20 minutes after pressurization, to allow for equilibration (see [9] for a discussion about the kinetics of xenon binding) and was completed within 4 h. Data sets were processed with the MOSFLM program [35] interfaced with the CCP4 package [36]. Lorentz-polarization corrections were applied to all intensity measurements. The various frames were scaled together by applying overall and resolution-dependent scale factors. The derivative data were scaled to the native by applying overall scale and anisotropic temperature factors.

The coordinates of the refined complexes of xenon with PPE and HLC will be deposited in the Brookhaven protein data bank [11].

Acknowledgements: We thank Arnaud Ducruix and Bernadette Arnoux (LBS, Gif sur Yvette, France) for continuing interest in this study, for their help in providing us with crystals of HLC and for providing us with the coordinates of the refined structure of HLC prior to publication. We are also grateful to Nathalie Colloc'h, Jacques Chomilier and Jean-Paul Mornon (LMCP, Paris, France) for their constant interest and for their commitment to participate at various stages of this project.

References

1. Wilhelm, E., Battino, R. & Wilcock, J. (1977). Low-pressure solubility of gases in liquid water. *Chem. Rev.* **77**, 219–259.
2. Cullen, E. & Gross, G. (1951). Anesthetic properties of xenon in animals and human beings, with additional observations on krypton. *Science* **113**, 580–582.
3. Atkins, H.L. (1975). Radiopharmaceuticals. *Phys. Rep.* **21**, 315–367.
4. Albert, M.S., *et al.*, & Wishnia, A. (1994). Biological magnetic resonance imaging using laser-polarized ^{129}Xe. *Nature* **370**, 199–201.
5. Cramer, F. & Henglein, F.M. (1957). Verbindungen von α-cyclodextrin mit Gasen. *Chem. Ber.* **90**, 2572–2575.
6. Schoenborn, B.P., Watson, H.C. & Kendrew, J.C. (1965). Binding of xenon to sperm whale myoglobin. *Nature* **207**, 28–30.
7. Schoenborn, B.P. (1965). Binding of xenon to horse haemoglobin. *Nature* **208**, 760–762.
8. Vitali, J., Robbins, A.H., Almo, S.C. & Tilton, R.F. (1991). Using xenon as a heavy atom for determining phases in sperm whale metmyoglobin. *J. Appl. Crystallogr.* **24**, 931–935.
9. Schiltz, M., Prangé, T. & Fourme, R. (1994). On the preparation and X-ray data collection of isomorphous xenon derivatives. *J. Appl. Crystallogr.* **27**, 950–960.
10. Bode, W. & Huber, R. (1986). Serine proteases. In *Molecular and Cellular Basis of Digestion.* (Desnuelle, P., Sjostrom, H. & Noren, O. eds), pp. 213–234, Elsevier, Amsterdam.
11. Bernstein, F.C., *et al.*, & Tasumi, M. (1977). The protein data bank: a computer-based archival file for macromolecular structures. *J. Mol. Biol.* **112**, 535–542.

12. Broutin, I. (1993). Affinement de la structure de la collagenase d'*Hypoderma Lineatum*. [PhD thesis], Université Paris-Sud, France.
13. Arnoux, B., Broutin, I., Pascard, C., Ducruix, A. & LeCroisey, A. (1993). 1.8 Å crystal structure of collagenase from insect larvae *Hypoderma lineatum*. *Acta Crystallogr. A* **49S**, 84.
14. Brünger, A.T., Krukowski, A. & Erickson, J.W. (1990). Slow-cooling protocols for crystallographic refinement by simulated annealing. *Acta Crystallogr. A* **46**, 585–593.
15. Brünger, A.T. (1988). *X-PLOR Manual*. Department of Molecular Biophysics and Biochemistry, Yale University, New Haven, CT. USA.
16. Konnert, J.H. & Hendrickson, W.A. (1980). A restrained parameter thermal factor refinement procedure. *Acta Crystallogr. A* **36**, 344–350.
17. Tilton, R.F., Kuntz, I.D. & Petsko, G.A. (1984). Cavities in proteins: structure of a metmyoglobin–xenon complex solved to 1.9 Å. *Biochemistry* **23**, 2849–2857.
18. Kraut, J. (1977). Serine proteases: structure and mechanism of catalysis. *Annu. Rev. Biochem.* **46**, 331–358.
19. Meyer, E., Cole, G., Radhakrishnan, R. & Epp, O. (1988). Structure of native porcine pancreatic elastase at 1.65 Å resolution. *Acta Crystallogr. B* **44**, 26–38.
20. Takahashi, L.H., Radhakrishnan, R., Rosenfield, R.E.Jr., Meyer, E.F. & Trainer, D.A. (1992). Crystal structure of the covalent complex formed by a peptidyl α,α-difluoro-β-keto amide with porcine pancreatic elastase at 1.78 Å Resolution. *J. Am. Chem. Soc.* **111**, 3368–3374.
21. Tilton, R.F., *et al.*, & Kollman, P.A. (1986). Computational studies of the interaction of myoglobin and xenon. *J. Mol. Biol.* **192**, 443–456.
22. Wright, C.S., Alden, R.A. & Kraut, J. (1969). Structure of subtilisin BPN' at 2.5 Å resolution. *Nature* **221**, 235–242.
23. Drenth, J., Hol, W.G.J., Jansonius, J.N. & Koekoek, R. (1972). Subtilisin Novo — the three-dimensional structure and its comparison with Subtilisin BPN'. *Eur. J. Biochem.* **26**, 177–181.
24. Robertus, J.D., *et al.*, & Wilcox, P.E. (1972). An X-ray crystallographic study of the binding of peptide chloromethyl ketone inhibitors to subtilisin BPN'. *Biochemistry* **11**, 2439–2449.
25. Pollack, G.L. (1964). Solid state of rare gases. *Rev. Mod. Phys.* **36**, 748–791.
26. Tilton, R.F. & Kuntz, I.D. (1982). Nuclear magnetic resonance studies of xenon-129 with myoglobin and hemoglobin. *Biochemistry* **21**, 6850–6857.
27. Miller, K.W., *et al.*, & Williamson, K.L. (1981). Xenon NMR: chemical shifts of a general anesthetic in common solvents, proteins and membranes. *Proc. Natl. Acad. Sci. USA* **78**, 4946–4949.
28. Martinez, C., De Geus, P., Lauwereys, M., Mathissens, G. & Cambillau, C. (1992). *Fusarium solani* cutinase is a lypolytic enzyme with a catalytic serine accessible to solvent. *Nature* **356**, 615–618.
29. Ollis, D.L., *et al.*, & Goldman, A. (1992). The α/β hydrolase fold. *Protein Eng.* **5**, 197–211.
30. Shotton, D.M., *et al.*, & Rao, L. (1968). Crystalline porcine pancreatic elastase. *J. Mol. Biol.* **32**, 155–156.
31. Petsko, G.A. & Tsernoglou, D. (1976). The structure of subtilopeptidase, I. X-ray crystrallographic data. *J. Mol. Biol.* **106**, 453–456.
32. LeCroisey, A., Boulard, C. & Keil, B. (1979). Chemical and enzymatic characterisation of the collagenase from insect *Hypoderma lineatum*. *Eur. J. Biochem.* **101**, 385–393.
33. Ducruix, A., Arnoux, B., Pascard, C., LeCroisey, A. & Keil, B. (1981). Crystallization and preliminary X-ray diffraction data for the collagenase of *Hypoderma lineatum* larvae. *J. Mol. Biol.* **151**, 327–328.
34. Fourme, R., *et al.*, & Frouin, J. (1992). Bent crystal, bent multilayer optics on a multipole wiggler line for an X-ray diffractometer with an imaging plate detector. *Rev. Sci. Instrum.* **63**, 982–987.
35. Leslie, A. (1994). *Mosflm User Guide, Mosflm version 5.20*. MRC Laboratory of Molecular Biology, Cambridge, UK.
36. Collaborative Computational Project, Number 4 (1994). The CCP4 suite: Programs for protein crystallography. *Acta Crystallogr. D* **50**, 760–764.

Received: **22 Dec 1994**; revisions requested: **17 Jan 1995**; revisions received: **30 Jan 1995**. Accepted: **8 Feb 1995**.